RSC Advances

PAPER

View Article Online
View Journal | View Issue

Cite this: *RSC Adv.*, 2021, **11**, 40140

Low molecular weight glycerol derived coatings on magnetic nanoparticles: role of initiator, temperature, rate of monomer addition, enhanced biocompatibility and stability†

Simon Doswald and Wendelin Jan Stark *

Biocompatible polymer coatings for magnetic nanoparticles have shown to drastically increase their usability towards biomedical applications. The coatings imprint characteristics such as stability, resistance to non-specific adsorption and tolerance in complex media for biomedicine. Herein, a thorough investigation towards the anionic ring-opening polymerization of glycidol on the surface of carbon-coated cobalt nanoparticle was performed. Reaction parameters that influence polymer growth have been investigated. Thereafter, a maximal achievable hyperbranched polyglycidol M_w of up to 1148 g mol^{-1} under optimal reaction conditions was obtained. With this coating, the dispersion stability of the particles could be substantially increased, the non-specific adsorption of proteins could be decreased to 10% while retaining an efficient magnetic separation.

Received 4th May 2021
Accepted 27th November 2021

DOI: 10.1039/d1ra03475h

rsc.li/rsc-advances

Introduction

Magnetic nanoparticles have been extensively used towards biotechnical and biomedical applications in the last decades. Metal or metal oxide nanoparticles have been prepared for applications such as diagnostics, drug delivery, hyperthermia or the removal of toxins or cells from blood.[1] Throughout the stated applications there are factors to consider, when dealing with *in vitro* or *in vivo* experiments such as cytotoxicity, blood compatibility, stability or biological fate.[2,3] With these restrictions, a lot of the metal or metal oxide nanoparticles become unavailable or unusable for the aforementioned applications. Even though, they might possess other beneficial attributes (*e.g.* the high magnetic saturation of carbon-coated metallic nanoparticles),[4] that may be well worth exploring further. Therefore, such particles need to be engineered in order to amend for their limited capabilities towards biocompatibility and stability.

One widely explored option is to coat the nanoparticles with a biocompatible compound, also called "stealth coating", that can change the characteristics of the nanoparticle towards the desired application.[5] Since the introduction of dextran as a possible coating of nanoparticles,[6] numerous polymers, natural and synthetic, have been applied onto nanoparticles in various studies. There are two general approaches to coat a particle, graft-to and graft-from. The graft-to method refers to the use of a polymer that is then directly linked onto the surface of the particle. Graft-from refers to the direct polymerization of a monomer onto the particle surface and therefore, gradually create a coating surrounding the particle (Fig. 1). With the graft-to method dense coatings with a high molecular weight are challenging to achieve, as each attached polymer on the surface raises the activation barrier for other polymers to react on the surface, due to the increased steric hindrance. The graft-from method seems to be less hindered by this fact, as a coating is gradually created and the used monomers are small and less hindered mobility wise. Nevertheless, the challenge here lies as well in research of monomers and reactions that are active

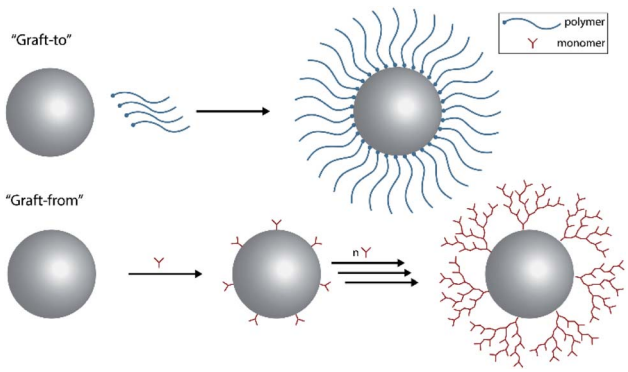

Fig. 1 Illustration of the two covalent coating methods of nanoparticles. "Graft-to" on the example of a linear polymer anchored onto the nanoparticle and "graft-from" on the example of a surface initiated hyperbranched polymerization.

Departement of Chemistry and Applied Science, Institute of Chemical Engineering and Biosciences, ETH Zurich, Vladimir-Prelog-Weg 1, 8093 Zurich, Switzerland. E-mail: wstark@ethz.ch

† Electronic supplementary information (ESI) available. See DOI: 10.1039/d1ra03475h

enough to achieve a reasonable surface-polymerization rate on the nanoparticle.

A very prominent polymer used for coatings in biomedicine is polyethylene glycol (PEG). This polymer provides a highly hydrophilic character, as the inclusion of water into the coating is possible (*i.e.* hydrogels). Additionally, PEG resists non-specific adsorption of proteins well and shows good tolerance towards biocompatibility. Therefore, PEG-conjugated nanoparticles have been widely applied and are considered as sort of a gold standard for biocompatible coatings.[7]

A polymer very similar to PEG is polyglycidol (PG), which is subject to this study. It is shown in recent articles that PG exhibits comparable or even higher biocompatibility than PEG.[8–10] Polyglycidol can be synthesized linearly and hyperbranched, whereas it was shown that both polymer variants behave similarly towards biocompatibility.[11] Hyperbranched polyglycidol (HPG) can be easily synthesized onto surfaces *via* anionic ring opening polymerization (ROP) of glycidol. The hyperbranched architecture allows for abundant reactive hydroxyl groups for variable functionalization and the resulting coating shows good characteristics towards stability in solution due to the high solubility of the hydroxyl network and excellent resistance towards non-specific adsorption of proteins. The coating of magnetic nanoparticles with HPG has recently generated a lot of interest in biomedicine due to the simplicity in synthesis and improved characteristics of the coated magnetic nanoparticles.[12–14] Different applications for HPG coated magnetic nanoparticles have been developed. First, such HGP coated magnetic nanoparticles may be used as MRI contrast agents as shown by Arsalani and coworkers.[15] The functionalization of HPG coated iron oxide with RGD, a cyclic peptide, to target specific cancer cells was developed by Zhao and coworkers.[16] Differently, Moorthy *et al.* conjugated HPG coated iron oxide nanoparticles with 5-FU, an anticancer drug, to show possible use of the magnetic nanoparticle conjugate as a drug delivery vehicle.[17]

All these applications profit from the HPG coating of the magnetic nanoparticles, due to the increased stability and the reduced non-specific adsorption. Nevertheless, in the articles about the improved characteristics or the applications of the HPG coated magnetic nanoparticles, there is no clear statement about the coating thickness or polymer length. With increased coating thickness, there are inherently better capabilities towards resistance to non-specific adsorption and stability in solution. If the magnetic particles are to be used as a scavenger to remove for example toxins from blood,[18,19] the separability from solution becomes crucial as it needs to be not only effective but also time efficient.[20] Therefore, there is a balance, where an optimal coating thickness can be elaborated, that shows good stability and resistance to non-specific adsorption and the particles can still be efficiently removed.

In this article, the anionic ROP of glycidol was investigated testing different reaction parameters to elaborate coating thickness of HPG surface functionalized on carbon-coated cobalt (CCo) nanoparticles. The HPG coating of different chain lengths on the CCo nanoparticles were then subjected to three tests; resistance to non-specific adsorption, stability in solution and magnetic separation from solution.

Experimental

Materials

All commercially available reagents were procured from Sigma-Aldrich and used as received if not otherwise stated. Carbon-coated cobalt nanoparticles were kindly received from Turbobeads Ltd. Information about the size distribution of the particles can be found in Grass *et al.*[21] The functionalized nanoparticles were analyzed by FT-IR spectroscopy (5% in KBr) and elemental microanalysis (ELEMENTAR, Mikroanalysensysteme).

Synthesis of initiators: CCo–PhEtOH and CCo–PhOH

Synthesis was adapted from Grass *et al.*[4] and the reaction is depicted in Scheme 1. Twenty-five grams CCo nanoparticles were dispersed with an ultrasonic bath in 300 mL H_2O. 3.5 g (25.5 mmol) 4-aminophenethyl alcohol (or 4-aminophenyl alcohol respectively) were dissolved in 50 mL H_2O and 10 mL hydrochloric acid. This solution was added to the dispersed particle solution. Separately, 3.5 g (50.7 mmol) $NaNO_2$ was dissolved in 30 mL H_2O in an ice bath and then also added slowly to the particle solution. The reaction was carried out for one hour in an ultrasonic bath at room temperature. The resulting particles were washed by dispersing them in 300 mL of each 3× deionized H_2O, 3× ethanol, 3× acetone. The particles were each time dispersed for five minutes in an ultrasonic bath and separated with a commercial neodymium magnet. The resulting particles were dried under *vacuo* at 50 °C overnight.

Synthesis of CCo–HPG

Synthesis was adapted from literature[12,22] and depicted in Scheme 1. In a typical reaction, 0.6 g CCo–PhEtOH particles were dispersed in 10 mL of a dry 2 M NaOMe/MeOH solution in a two neck 100 mL round bottom flask by ultrasonication for 20 minutes and then subsequently stirred vigorously for another

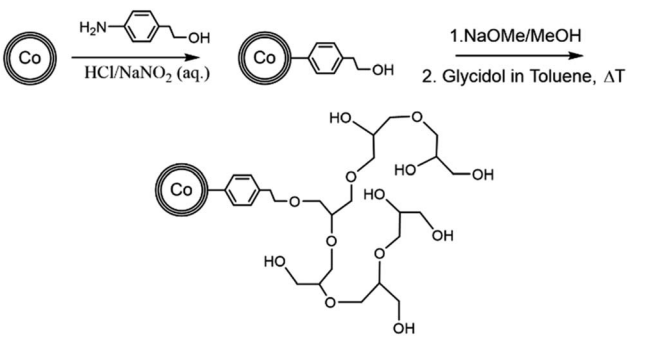

Scheme 1 Synthesis pathway for the HPG coating of CCo nanoparticles. First, the bare CCo nanoparticles are functionalized with an amino phenethyl alcohol by diazotization. Then the particles were deprotonated and reacted with glycidol to achieve the HPG coating on the surface.

40 minutes under N_2 atmosphere. The particles were subsequently washed four times with 10 mL dry methanol by dispersing the particles in an ultrasonic bath for five minutes and magnetic separation. Finally, the particles were dried under *vacuo*. The dried particles were dispersed in 20 mL dry toluene in an ultrasonic bath under N_2. The toluene-particle slurry was brought to reaction temperature and 10 mL glycidol (10 mL h^{-1}) was added *via* syringe pump. The typical reaction was performed for 16 hours after start of the glycidol addition. Afterwards, the HPG coated CCo particles were magnetically separated from the solution. The resulting particles were washed with each 20 mL; 1× toluene, 1× ethanol, 3× H_2O, 3× methanol by sonication for five minutes and magnetic separation and then dried under *vacuo* at 50 °C overnight.

Adsorption experiment with BSA–fluorescein conjugate

A 2 mg mL^{-1} solution of the different HPG coated CCo nanoparticles (M_w (g mol^{-1}): CCo (blank), 0, 209, 451, 825, 1148) was prepared in PBS (pH: 7.4, Gibco) by ultrasonication. Separately, a 0.1 mg mL^{-1} solution of a bovine serum albumin–fluorescein conjugate (BSA–fluorescein) was prepared. Then, each 500 μL of the particle dispersion and BSA–fluorescein solution were added together and incubated at room temperature for one hour at 900 rpm in an orbital shaker. Next, the particles were removed from the solution with the help of a magnet and the solution was measured in triplicates in a TECAN reader (ex: 485, em: 535).

Sedimentation and magnetic separation experiments

Solutions of the HPG coated CCo nanoparticles (M_w (g mol^{-1}): CCo (blank), 0, 209, 451, 825, 1148) were prepared with a concentration of 1 mg mL^{-1}, 4 mL total. Each solution was dispersed in an ultrasonic bath for five minutes and then either set up for sedimentation or placed close to a strong magnet for magnetic separation. The time evolution was recorded with a Canon digital camera and image analysis for the time evolution was done with ImageJ.

Results & discussion

The anionic polymerization of glycidol on phenylethanol and phenol functionalized carbon-coated cobalt nanoparticles was investigated and conditions for optimal surface growth were explored. The obtained HPG coated magnetic nanoparticles with different polymer chain lengths on the surface were then tested towards separability, stability and non-specific adsorption of proteins. These are important characteristics towards the use of magnetic nanoparticles in biomedicine.

In a first set of experiments the influence of reaction parameters such as temperature, addition speed and change of initiator was investigated. As can be seen in Fig. 2A the anionically initiated surface polymerization is strongly dependent on the reaction temperature. Temperatures lower than 60 °C result in minimal surface polymerization. If the reaction temperature is increased from 60 °C to 95 °C, an almost linear increase in chain length can be observed. Surprisingly, when performing the surface polymerization at 110 °C, a decrease to a $M_w = 937$ g mol^{-1} was observed. To test the reaction at even higher temperatures we need to account for the boiling point of toluene (110 °C). A solvent exchange to *o*-xylene, which is chemically very similar to toluene, was used to perform the reaction at 140 °C. The resulting HPG coated CCo nanoparticles exhibited an even lower polymer chain length down to a M_w of 597 g mol^{-1}. Therefore, a side reaction may have taken place and seemed to be more prevalent at elevated temperatures. This will be discussed later on. Next, 1,4-dioxane and DMF were tested as possible alternative solvents for the surface polymerization of glycidol. In the case of 1,4-dioxane an average HPG length of 1059 g mol^{-1} units was achieved at 80 °C, meanwhile with DMF as solvent only about 56 g mol^{-1} was achieved, which means DMF seems to invoke further side reactions and seems to be unsuitable as a solvent for this type of polymerization.

In a next step the monomer addition speed was increased from full addition in 8 hours to full addition in 1 hour. As seen in Fig. 2B, the observed chain lengths in comparison to the results in Fig. 2A were slightly lower, this hints again at

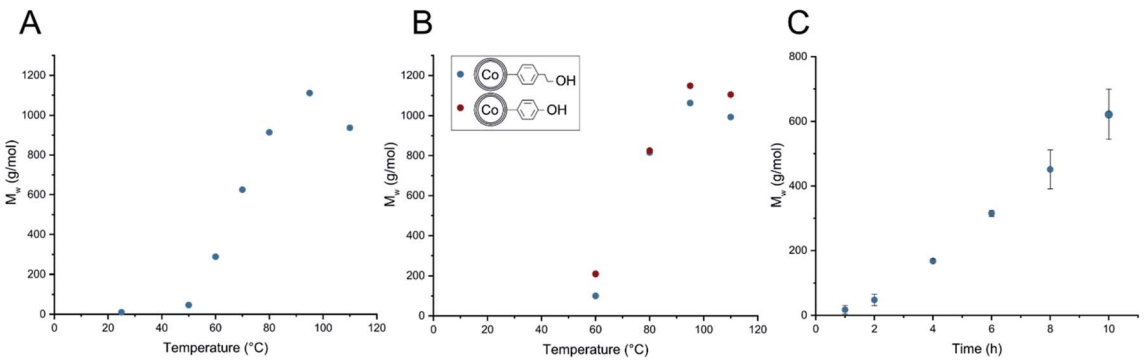

Fig. 2 Surface polymerization of glycidol onto CCo nanoparticles with different reaction parameters. (A) Temperature dependence of HPG growth, whereas monomer was added over 8 hours and total reaction time was 16 hours. (B) Temperature dependence of HPG growth of the two different initiators with monomer addition within one hour, total reaction time 16 hours. (C) Growth of surface polymerization over time at 80 °C, monomer addition within one hour. Calculation of polymer chain length functionalized on the magnetic nanoparticles can be found in ESI Appendix A2.†

a possible side reaction that may deplete monomer faster with an increased monomer concentration. In contrast, when decreasing the addition speed of the monomer in order that completion of addition is achieved in 16 hours, no further increase in polymer loading was observed. Additionally, there was only a small difference between CCo–PhEtOH and CCo–PhOH when used as initiators. Even though, they exhibit a difference in pK_a value, both functionalized nanoparticles were able to initiate the polymerization and achieve similar polymer chain length, this leads to believe that glycidol acts as a reactive or activated monomer in solution, which then favorably reacts with the active surface bound polymer chain. IR analysis indicates for both HPG functionalized nanoparticles typical IR bands for polyglycidol (C–H: 2850 cm^{-1} and C–O–C: 1100 cm^{-1}) were detected (Fig. 3). Further on, the surface chain growth over time was investigated. As depicted in Fig. 2C, the polymer chain growth progresses linearly, which supports a stepwise growth of the active polymer chain end on the nanoparticle surface.

As a next step, the reaction itself was investigated. The previous surface polymerizations have shown almost no surface reaction at temperatures below 60 °C and a decreased yield of surface polymerized glycidol at 110 °C and a substantial decrease at 140 °C (in *o*-xylene). This leads to the conclusion that the monomer needs activation energy to be in a state to be able to react and at high temperatures, competitive side reactions may occur, that deplete the glycidol and reduce maximal loading on the particle. As can be seen by an article of Weiss *et al.*,[23] it is possible for the spontaneous oligomerization of glycidol at elevated temperatures due to self-activation by hydrogen bonds from the alcohol towards the oxirane. Therefore, two possible polymerization reactions may occur in the investigated homogeneous reaction media. First, the intended reaction of the activated surface with the glycidol monomer, or secondly, the spontaneous oligomerization between two glycidol molecules as depicted in Scheme 2. Thus, as a next step, we wanted to investigate if and how this spontaneous oligomerization influences the anionic surface polymerization reaction, which hinders the production of high molecular weight coatings. Therefore, the supernatants after the polymerization at different temperatures were investigated with electron spray ionization mass spectroscopy. It was found that with an increase in temperature, the size of the largest detected oligomers increased significantly. For 70 °C, oligomers of up to 6 units (M + Na: 467.2099 g mol^{-1} ($C_{18}H_{36}O_{12}Na$)) were detected, at 80 °C up to 9 units (M + Na: 689.3199 g mol^{-1} ($C_{27}H_{54}O_{18}Na$)) and at 95 °C oligomers of up to 16 units (M + Na: 1207.5777 g mol^{-1} ($C_{48}H_{96}O_{32}Na$)) were detected in the respective supernatants. This coincides well with Weiss' article about a self-activated reaction of glycidol monomers with each other. Hence, a more pronounced starvation of monomer realistically takes place at elevated temperatures, which competitively hinders and suppresses the formation of high molecular weight coatings on the CCo nanoparticle surface for the herein used reaction pathway. Additionally, low temperature reactions show significantly lower surface polymerization than high temperature reactions and therefore extremely long reaction times would be needed to achieve a coating that may achieve more than the maximally obtained M_w of 1148 g mol^{-1}. The particles with a HPG M_w of 1148 g mol^{-1} were investigated with scanning transmission electron microscopy (STEM) and particle size distribution was determined (Fig. 4).

Further on, the reaction parameters were simplified, to appease for the fact the reaction occurs spontaneously between monomers, spontaneous reaction between surface alcohols of the nanoparticles and glycidol may occur as well. Therefore, surface polymerizations were performed without prior deprotonation of the hydroxyl groups on the nanoparticles. Additionally, the reaction was performed under non-inert conditions and adsorption of oligomerized glycidol (by heating over time) onto the magnetic nanoparticles was investigated as a control. In short, the surface reaction was still able to take place even without prior deprotonation and under non-inert conditions. The non-inert experiment and especially the adsorption experiment showed significant reduction in chain length (Table 1). In order to see if this is also applicable to different particles, thiol functionalized iron-oxide nanoparticles were prepared and subsequently used in the surface polymerization of glycidol

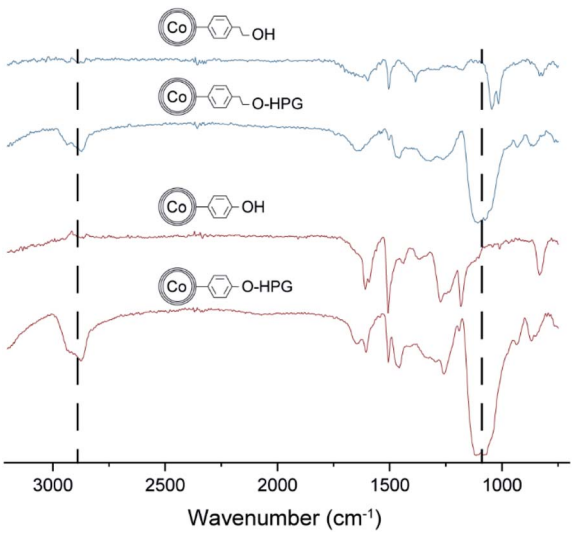

Fig. 3 IR spectra of the two different initiator particles CCo–PhEtOH, and CCo–PhOH and their corresponding HPG polymerized particles. IR bands: C–H (s): 2850 cm^{-1}, C–O–C (vs): 1100 cm^{-1}.

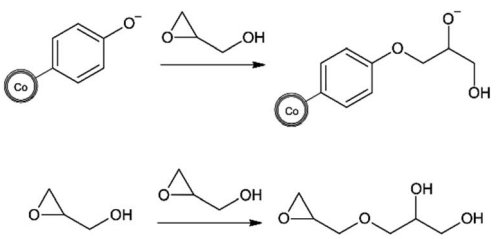

Scheme 2 Top: intended anionic surface reaction and subsequent polymerization on magnetic nanoparticles. Bottom: spontaneous oligomerization of glycidol in the homogeneous reaction mixture.

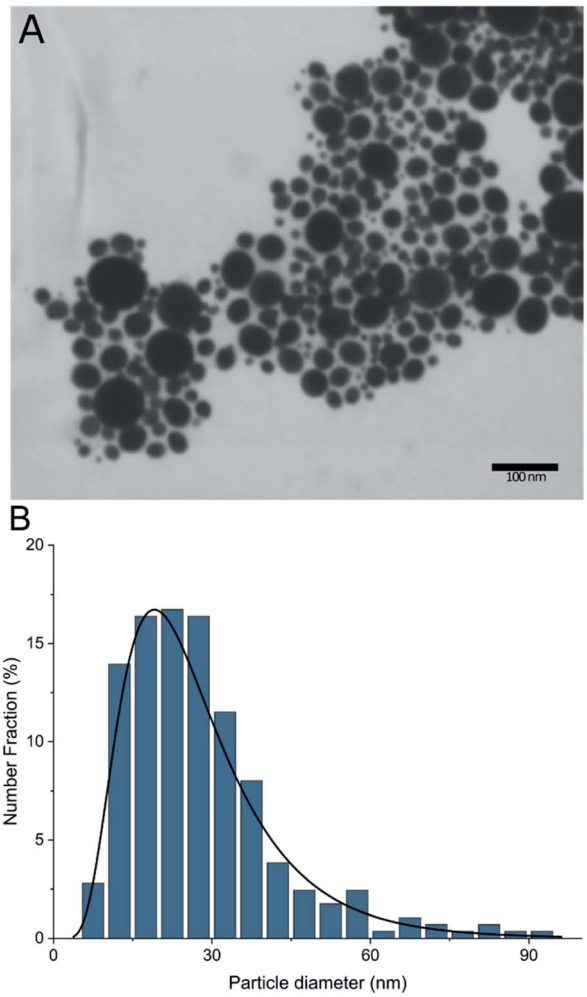

Fig. 4 (A) SEM image of HPG functionalized magnetic nanoparticles. (B) Particle size distribution of HPG functionalized particles with a M_w of 1148 g mol^{-1} from STEM imaging, 287 analysed particles and fitted with a log normal curve.

without prior deprotonation. The results showed polymerization also takes place to a similar degree with the iron-oxide nanoparticles (see Table S1 and Fig. S1† for detailed results). This means a simplification by leaving out the deprotonation step for the polymerization of glycidol on the surface of nanoparticles may be applicable to different particles than herein proposed or other surfaces in need of a simple and straightforward coating for the increase of biocompatibility. With this set-up of experiments, we were able to achieve a polyglycidol coating of up to 1148 g mol^{-1} on the nanoparticle surface. Coating efficiency seems to be mainly dependent on reaction temperature and time constraints.

When comparing this to other polymers used for an introduction of biocompatibility, the polymer length used is generally much larger. Therefore, we wanted to test if these low molecular weight HPG coated CCo nanoparticles may already show improved characteristics towards stability and biocompatibility, which are crucial for the use in biomedical applications.

Table 1 Investigation into change of deprotonation step in the anionic ROP synthesis of glycidol on the CCo nanoparticles at 80 °C. For the reactions without prior deprotonation, the particles were washed with toluene before the reaction set-up

Deviation of standard protocol	M_w of HPG on the surface of the nanoparticles (g mol^{-1})
NaOMe used to deprotonate (standard protocol)	813
LiOMe used to deprotonate	816
KOMe used to deprotonate	882
No deprotonation	637
No deprotonation, use non-inert conditions	500
Adsorption of oligomerized glycidol on CCo–PhEtOH particles	72[a]

[a] As calculated with previous method, but corresponds to physisorbed HPG oligomers on the magnetic nanoparticle surface.

Three characteristics were explored on the different coating thicknesses of the coated and the uncoated CCo nanoparticles. First, non-specific adsorption was investigated. This was done with the use of a fluorescein modified bovine serum albumin (BSA). Bovine serum albumin can be used as a simple model protein to show and investigate the non-specific adsorption of proteins. The second investigated feature was the magnetic separability. Efficient separation of the magnetic nanoparticles is important as time constraints may inhibit efficiency and dependent on application, full separation in a timely manner is crucial (*e.g.* clinical blood purification[24]). The final investigated characteristic was the stability of the coated nanoparticles in solution. Stability is needed, as the particles need to stay in solution long enough to ensure contact between nanoparticle and target for a reaction to take place (*e.g.* binding of a toxin). Since only mild dispersion methods should be used when handling biochemical compounds, harsh methods to easily disperse nanoparticles such as ultrasonication may harm the biochemical compounds. Therefore, the particles need to be easily dispersed and then stable long enough for reaction in solution. In order to investigate this trait, we looked at the sedimentation behavior over time of the particles to give some insights toward the stability of the differently coated CCo particles in solution.

Results of these three tests are summarized in Fig. 5. Non-specific adsorption of BSA is gradually decreased with an increased polymer length on the nanoparticles. Unfunctionalized CCo nanoparticles adsorb over 70% of the protein in solution. With the HPG coating a significant reduction can be observed. With only 1148 g mol^{-1} average HPG chain weight, non-specific adsorption of BSA could be reduced down to 10%, whereas with coatings lower than this, marginal further decrease in non-specific adsorption was observed. From M_w 0 to 451 g mol^{-1}, the coating seems to be ineffective in reducing non-specific adsorption, a M_w of at least around 825 g mol^{-1} is needed to have an observable effect. Afterwards, already a small

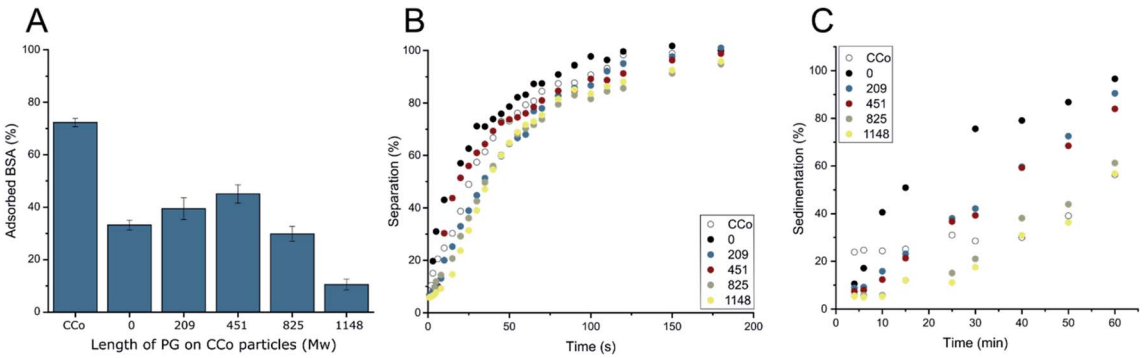

Fig. 5 Behavior of different low molecular weight hyperbranched polyglycidol coated CCo nanoparticles for different characteristics. Tested were particles with M_w 0, 209, 451, 825, 1148 g mol^{-1} units chain length and the unfunctionalized CCo nanoparticles. (A) Non-specific adsorption of BSA–fluorescein conjugate on the different magnetic nanoparticles. (B) Magnetic separation of the particles in PBS. (C) Sedimentation behavior of the particles in PBS.

increase in coating leads to significant improvements in anti-adhesive properties.

For the magnetic separability, the particles were dispersed by ultrasonication in PBS solution and separated with a strong magnet. This should simulate the efficiency of removal after a desired reaction or scavenge of a target is performed with the particles. Results of the separation tests can be found in Fig. 5B. Interestingly, in contrast to the non-specific adsorption experiment, the magnetic separation showed similar results for all the different coatings. There was no significant change even with the coating of 1148 g mol^{-1}. Complete separation was achieved for all the particles in under five minutes. On the other hand, the investigation of the dispersion stability of the different nanoparticles in PBS exhibited an observable difference between uncoated and the coated particles with up M_w of up to 1148 g mol^{-1} on the CCo nanoparticles (Fig. 5C). With 16 units polymerized on the nanoparticle surface the particles were able to stay well dispersed in solution for about 30 minutes, which should give enough contact time to perform possible reaction or capturing of a target in solution. Interestingly, when doing a magnetic separation and dispersion stability test in deionized water, drastic differences can be observed with the 16 units polymerized particles in contrast to the nanoparticles with a lower degree of polymerization (Fig. 6). With this, HPG coated magnetic nanoparticles were fabricated with a minimal molecular weight coating, that show increased resistance towards non-specific adsorption, a significantly increased stability in solution while still being able to be efficiently removed *via* magnetic separation.

In a last series of experiments different glycidyl derivates were investigated. The purpose was to find a simple way to incorporate functionalities other than alcohol groups directly into the backbone of the surface bound polymer. Five different derivatives were tested: allylglycidyl ether (AGE), glycidyl methacrylate (GMA), Boc-epoxypropylamine (BNG) and glycidyl trimethyl ammonium chloride (GTMA) and oxirane. Synthesis of the particles with AGE, GMA, BNG and oxirane did not result in a surface polymerization on the particles. Even a change in the deprotonation procedure with potassium *tert*-butanolate, or the use of triethylaluminum as a catalyst did not result in a reaction on the surface of the nanoparticles (Table 2). On the other hand, a reaction with GTMA as monomer resulted in an anchoring of a single GTMA unit on the surface of the nanoparticle.

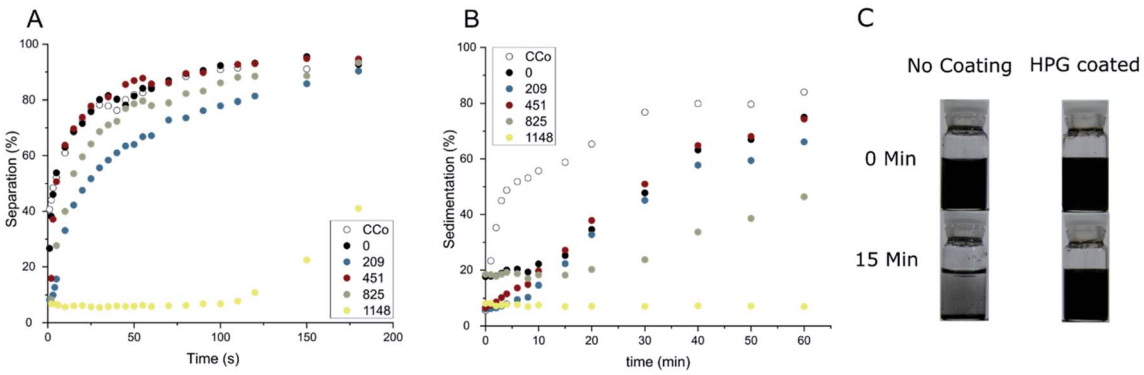

Fig. 6 Separation (A) and sedimentation (B) behaviour of the different magnetic nanoparticles in water. (C) Imaging of an uncoated and unstable magnetic nanoparticle solution and of a HPG coated (1148 g mol^{-1}) homogeneous and more stable magnetic nanoparticle solution just after sonication (0 min) and after 15 minutes.

Table 2 Test of different monomers: AGE, GMA, BNG, GTMA and oxirane

Monomer	Structure	Polymerization onto nanoparticles (Y/N)
Allylglycidyl ether	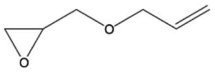	N
Glycidyl methacrylate	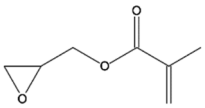	N
Boc-epoxypropylamine	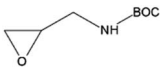	N
Oxirane		N
Glycidyl trimethyl ammonium chloride	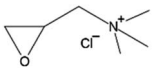	Y[a]

[a] Surface functionalization of one monomer unit.

This could be confirmed by element analysis (increase in N content) and a change in zeta-potential (from −16 to +34). The acquired magnetic nanoparticles functionalized with a single GTMA unit exhibited exceptional dispersion stability in aqueous solution for over 24 hours. Nevertheless, with these experiments it is displayed that the incorporation of new functionalities *via* direct polymerization seems to be challenging and post polymerization modification appears to be the more efficient and effective way for the introduction of new functionalities onto the HPG coated nanoparticles.

Conclusions

To summarize, the anionic ROP of glycidol was utilized to coat hydroxyl functionalized CCo nanoparticles. Reaction parameters such as temperature, addition speed and different initiators were investigated. It was found that at optimal conditions HPG with a M_w of up to 1148 g mol^{-1} was able to be anchored on the magnetic nanoparticles. Subsequently, the reaction itself was more closely investigated. It was found spontaneous oligomerization of glycidol in solution occurred at elevated temperature, which competes with the surface polymerization on the magnetic nanoparticles.

Further on, the as-obtained coated nanoparticles were tested towards the non-specific adsorption of proteins, separability from solution with a magnet and dispersion stability. The well coated magnetic nanoparticles have shown to drastically reduced non-specific adsorption of proteins down to only 10%, increased the stability in solution and retaining the efficient separation capabilities by magnet. Therefore, the ease of synthesis and exceptional qualities of the herein described nanoparticles display the need for a clear understanding about surface reaction mechanisms of biocompatible coatings. The herein performed study describes first steps towards defining the initial parameters needed to achieve efficient and effective surface coatings for later use in biomedical applications.

Conflicts of interest

W. J. S. declares a financial interest as he is a shareholder of Turbobeads LLC, a company producing magnetic nanoparticles.

Acknowledgements

Financial support by the ETH Zurich is kindly acknowledged. The authors thank Dr Elia M. Schneider for proof-reading the manuscript and the fruitful discussions and the MoBias Team for the ESI-MS measurements.

Notes and references

1 Q. A. Pankhurst, J. Connolly, S. K. Jones and J. Dobson, *J. Phys. D: Appl. Phys.*, 2003, **36**, R167–R181.
2 L. H. Reddy, J. L. Arias, J. Nicolas and P. Couvreur, *Chem. Rev.*, 2012, **112**, 5818–5878.
3 S. Doswald, W. J. Stark and B. Beck-Schimmer, *J. Nanobiotechnol.*, 2019, **17**, 73–83.
4 R. N. Grass, E. K. Athanassiou and W. J. Stark, *Angew. Chem., Int. Ed.*, 2007, **46**, 4909–4912.
5 N. Hadjesfandiari and A. Parambath, in *Engineering of Biomaterials for Drug Delivery Systems*, Elsevier, 2018, pp. 345–361.
6 R. Weissleder, H. C. Cheng, A. Bogdanova and A. Bogdanov, *J. Magn. Reson. Imaging*, 1997, **7**, 258–263.
7 J. S. Suk, Q. Xu, N. Kim, J. Hanes and L. M. Ensign, *Adv. Drug Delivery Rev.*, 2016, **99**, 28–51.
8 M. Imran Ul-Haq, B. F. L. Lai, R. Chapanian and J. N. Kizhakkedathu, *Biomaterials*, 2012, **33**, 9135–9147.
9 M. Imran ul-haq, B. F. L. Lai and J. N. Kizhakkedathu, *Macromol. Biosci.*, 2014, **14**, 1469–1482.
10 A. S. Abu Lila, K. Nawata, T. Shimizu, T. Ishida and H. Kiwada, *Int. J. Pharm.*, 2013, **456**, 235–242.
11 R. K. Kainthan, J. Janzen, E. Levin, D. V. Devine and D. E. Brooks, *Biomacromolecules*, 2006, **7**, 703–709.
12 S. Wang, Y. Zhou, S. Yang and B. Ding, *Colloids Surf., B*, 2008, **67**, 122–126.
13 L. Zhou, C. Gao and W. Xu, *Langmuir*, 2010, **26**, 11217–11225.
14 L. Wang, D. Su, L. Zeng, N. Liu, L. Jiang, X. Feng, K. G. Neoh and E. T. Kang, *Dalton Trans.*, 2013, **42**, 13642–13648.
15 N. Arsalani, H. Fattahi, S. Laurent, C. Burtea, L. Vander Elst and R. N. Muller, *Contrast Media Mol. Imaging*, 2012, **7**, 185–194.
16 L. Zhao, T. Chano, S. Morikawa, Y. Saito, A. Shiino, S. Shimizu, T. Maeda, T. Irie, S. Aonuma, H. Okabe, T. Kimura, T. Inubushi and N. Komatsu, *Adv. Funct. Mater.*, 2012, **22**, 5107–5117.

17 M. S. Moorthy, Y. Oh, S. Bharathiraja, P. Manivasagan, T. Rajarathinam, B. Jang, T. T. Vy Phan, H. Jang and J. Oh, *RSC Adv.*, 2016, **6**, 110444–110453.
18 I. K. Herrmann, A. Schlegel, R. Graf, C. M. Schumacher, N. Senn, M. Hasler, S. Gschwind, A. M. Hirt, D. Günther, P. A. Clavien, W. J. Stark and B. Beck-Schimmer, *Nanoscale*, 2013, **5**, 8718–8723.
19 I. K. Herrmann, M. Urner, S. Graf, C. M. Schumacher, B. Roth-Z'graggen, M. Hasler, W. J. Stark and B. Beck-Schimmer, *Adv. Healthcare Mater.*, 2013, **2**, 829–835.
20 L. Bougas, L. D. Langenegger, C. A. Mora, M. Zeltner, W. J. Stark, A. Wickenbrock, J. W. Blanchard and D. Budker, *Sci. Rep.*, 2018, **8**, 3491–3498.
21 R. N. Grass and W. J. Stark, *J. Mater. Chem.*, 2006, **16**, 1825–1830.
22 M. Khan and W. T. S. Huck, *Macromolecules*, 2003, **36**, 5088–5093.
23 M. E. R. Weiss, F. Paulus, D. Steinhilber, A. N. Nikitin, R. Haag and C. Schütte, *Macromol. Theory Simul.*, 2012, **21**, 470–481.
24 I. K. Herrmann, M. Urner, F. M. Koehler, M. Hasler, B. Roth-Z'graggen, R. N. Grass, U. Ziegler, B. Beck-Schimmer and W. J. Stark, *Small*, 2010, **6**, 1388–1392.